JPE 18-6-28

https://doi.org/10.6113/JPE.2018.18.6.1920
ISSN(Print): 1598-2092 / ISSN(Online): 2093-4718

Step-Up Asymmetrical Nine Phase Delta-Connected Transformer for HVDC Transmission

Arafet Ben Ammar† and Faouzi Ben Ammar*

†Laboratory of Materials, Measurements and Applications, National School of Engineering of Tunis, University of Tunis, Tunis, Tunisia
*Laboratory of Materials, Measurements and Applications, National Institute of Applied Sciences and Technology, University of Carthage, Tunis, Tunisia

Abstract

In order to provide a source for nine phases suitable for 18-pulse ac to dc power, this paper proposes a new structure for a step-up asymmetrical delta-connected transformer for converting three-phase ac power to nine-phase ac power. The design allows for symmetry between the nine output voltages to improve the power quality of the supply current and to minimize the THD. The results show that this new structure proves the equality between the output voltages with 40°- α and 40°+ α phase shifting and produces symmetrical output currents. This result in the elimination of harmonics in the network current and provides a simulated THD that is equal to 5.12 %. An experimental prototype of the step-up asymmetrical delta-autotransformer is developed in the laboratory and the obtained results give a network current with a THD that is equal to 5.35%. Furthermore, a finite element analysis with a 3D magnetic field model is made based on the dimensions of the 4kVA, 400 V laboratory prototype three-phase with three-limb delta-autotransformer with a six-stacked-core in each limb. The magnetic distribution flux, field intensity and magnetic energy are carried out under open-circuit operation or load-loss.

Key words: 18-pulse ac-dc converters, Asymmetrical autotransformer, LCC-HVDC, Thyristor, THD current

I. INTRODUCTION

Most of the HVDC systems in operation today are based on Line-Commutated Current-Sourced Converters (LCC/CSC) with 6, 12, 18 or 24-pulse converters [1]. In fact, 6-pulse Thyristor-converters [2] are the most commonly used. However, this basic configuration generates (6k ± 1) harmonics in the current network with amplitudes above the recommended limits of the IEEE 519 standard. To improve the THD, the 12-pulse converter [3], [4] is made up of two 6-pulse-converters associated in parallel with the autotransformer through two sets of three phase voltages phase shifted +15° and -15° with respect to the supply voltages. This configuration produces (12k±1) harmonics in the current network with 5 and 7 harmonics cancellation. The 18-pulse converter [5], [6] is composed of three 6-pulse-converters parallel fed with an autotransformer with three sets of three phases voltages phase shifted (+40° 0 -40°) or (-20° 0 20°) with respect to the supply voltages. This system arrangement produces (18k±1) harmonics order in the current network with 5, 7, 11 and 13 harmonics cancellation in accordance with IEEE 519 requirements.

Recently, the Modular Multilevel voltage source Converter (MMC) has been realized for HVDC projects. The MMC is a serial connection of several independent voltage source IGBT converter submodules, each containing its own storage capacitor [7]. A typical MMC for an HVDC application contains around 300 submodules [8] connected in series creating a 301 voltage level converter with subsequent a improvement of the current THD in the network connection. There are two main drawbacks in MCC-HVDC technology. The first drawback is the complex hardware and software to control the large number of IGBTs. In addition, is not easy to balance the capacitor source voltage for each of the submodules. The protection concern is identified as the second principal drawback of emerging MMC-HVDC technology [9],

Manuscript received Mar. 30, 2017; accepted Apr. 16, 2018
Recommended for publication by Associate Editor Seon-Hwan Hwang.
†Corresponding Author: arafet.ammar@hotmail.fr
Tel: +216-21620403956, University of Tunis
*Lab. of Materials, Measurements and Applications, National Institute of Applied Sciences and Technology, University of Carthage, Tunisia

[10]. In fact, the over current and over voltage problems caused by DC line faults compromise the security of (MMC-HVDC). Thus, the identification, classification and post-fault system recovery response should be improved. Conventional VSCs and half-bridge MMC topologies are highly susceptible to DC side short circuit faults due to the behavior of the antiparallel diodes of the IGBTs [11].

The greater part of power transmission is assured by means of the Line-Commutated Current-Sourced LCC-HVDCs and it has become an industry standard. Thyristor based LCC-HVDC technology has a higher blocking voltage capability when compared to the IGBT semiconductors in MCC-HVDC technology. The high power Thyristor has been an unsurpassed component in LCC-HVDC converters for the past several decades that is still being developed for new LCC-HVDC projects and its reliability has been proven by more than thirty installations worldwide [12], [13]. For example, ABB has developed a 6-inch Thyristor with an 8500V/4000A capability. Siemens has more than 30 years of experience in the development and manufacturing of highly reliable Thyristors by introducing new advanced concepts such as water cooling, corrosion-free and self-protecting direct-light-triggered capabilities [14].

For LCC-HVDC applications, numerous transformers and autotransformers are available to reach 18-pulse structure, star connected, delta-connected and polygon connected autotransformers [15].

Firstly, the insulation transformers must be evaluated for the required full power on the primary and secondary windings. Secondly, the insulation transformers are relatively large to result in the separation between the primary and secondary windings. When isolation between the grid and the rectifier is not necessary, the use of an autotransformer consisting of a relative majority of series and common windings has an advantage for reducing the dimensions, mass and cost of the three-phase conversion.

In this paper, a new step-up asymmetrical nine phase delta-autotransformer is presented. This paper is structured as follows. Section II presents the system configuration and several structures for the symmetrical and asymmetrical delta-connected transformer used for HVDC systems, which provide equality between the nine output voltages and harmonic elimination in the network sides of the two ac stations. In Section III, a mathematical analysis based on a phasor diagram of the design of the proposed step-up asymmetrical nine phase delta autotransformer is presented. Section IV presents an experimental prototype of the autotransformer, geometric construction of the core and windings and a finite element analysis (FEA) using ANSYS Maxwell 2D, 3D. Simulation results of the topology of the 18-pulse are discussed and validated with the experimental prototype in Section V. An HV autotransformer design is presented in Section VI. Finally, some concussions are presented in Section VII.

II. System Configuration

A schematic diagram of an HVDC system with an 18-pulse ac–dc Thyristor converter is shown in Fig. 1. This structure needs the design of an autotransformer with special couplings. A symmetric delta-connected transformer is developed where the nine output voltages have 40° phase shifting with the three supply voltages.

The delta-connected transformer that proved the conventional 3/9 transformation is shown in Fig. 1. The nine created output voltages have an rms voltage that is identical to the supply voltages. However, the rms currents are different because the main converter is fed directly from the line and is higher than the current of the auxiliary converters that are fed through the short autotransformer windings, which are characterized by some leakage inductance. This structure has the disadvantage of a large circulating of the third harmonic current which raises the transformer kVA rating [16]. The interphase reactors have an objective to connect the positive and negative terminals of the three converters to provide a parallel connection between them as shown in Fig. 1. As a result, each converter operates as an independent 6-pulse converter with 120° electrical conduction angles [17].

One solution to ensure symmetry between the nine output voltages and the inputs current of the three converters is inserting an auxiliary reactance before the main converters resulting a network current with fewer harmonics. The value of this auxiliary reactance is similar to the transformer leakage impedance feeding the auxiliary rectifiers [17].

Another solution to the problems of sharing current between the three converters is to provide an autotransformer that correspondingly spaces the output voltages in phase. This autotransformer contains 18 windings (6 windings per phase), and the 6th winding is for reducing the amplitude of the input current for the main converter.

There are several existing structures for the extended winding connection to an autotransformer, including an autotransformer having serial windings that form a delta while from the same coil there are extension windings magnetically coupled with an inappropriate phase shift angle [19]. An autotransformer with a 40° phase shifting has a three-phase input connected to a delta configuration via auxiliary windings to provide equality between the nine output voltages [20].

III. Design of the New Step-Up Asymmetrical Nine Phase Autotransformer

As shown in Fig. 3, a step-up delta-connected autotransformer is designed where (V_A, V_B, V_C) are the phase AC inputs and (V_a, V_b, V_c), (V_{11}, V_{12}, V_{13}) and (V_{21}, V_{22}, V_{23}) are the nine phase AC outputs, where all of the voltages have an identical magnitude. The three voltages (V_a, V_b, V_c) are

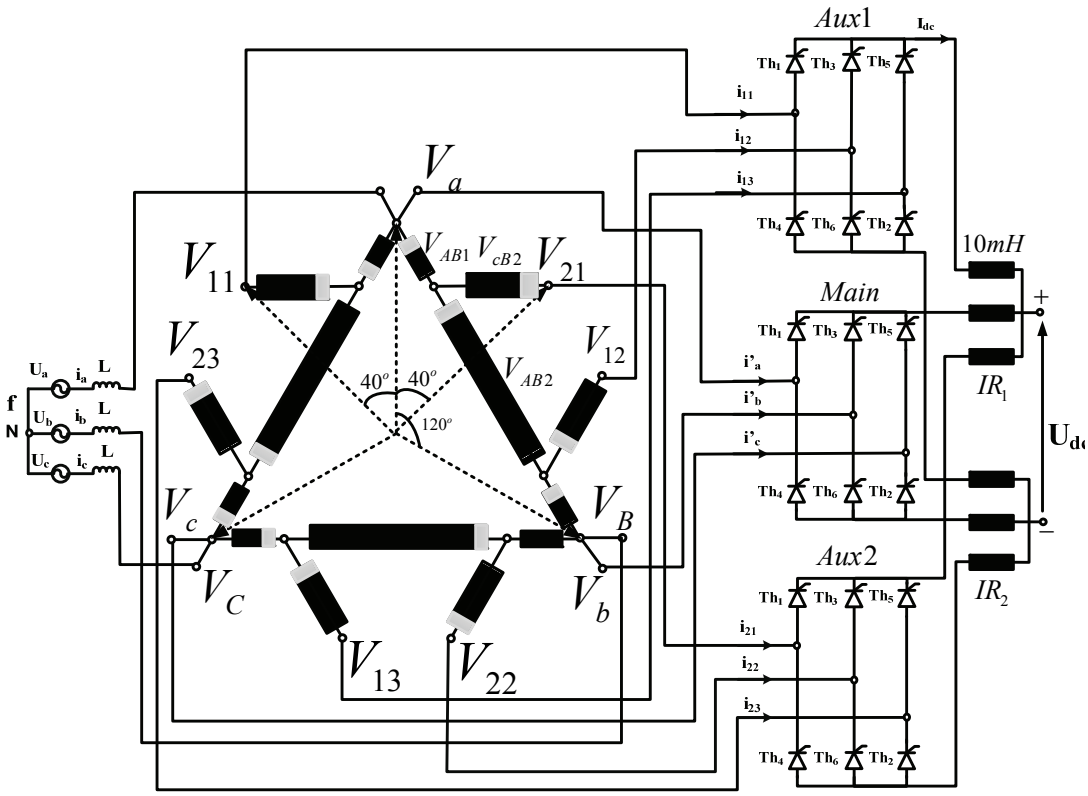

Fig. 1. Symmetrical delta-connected autotransformer.

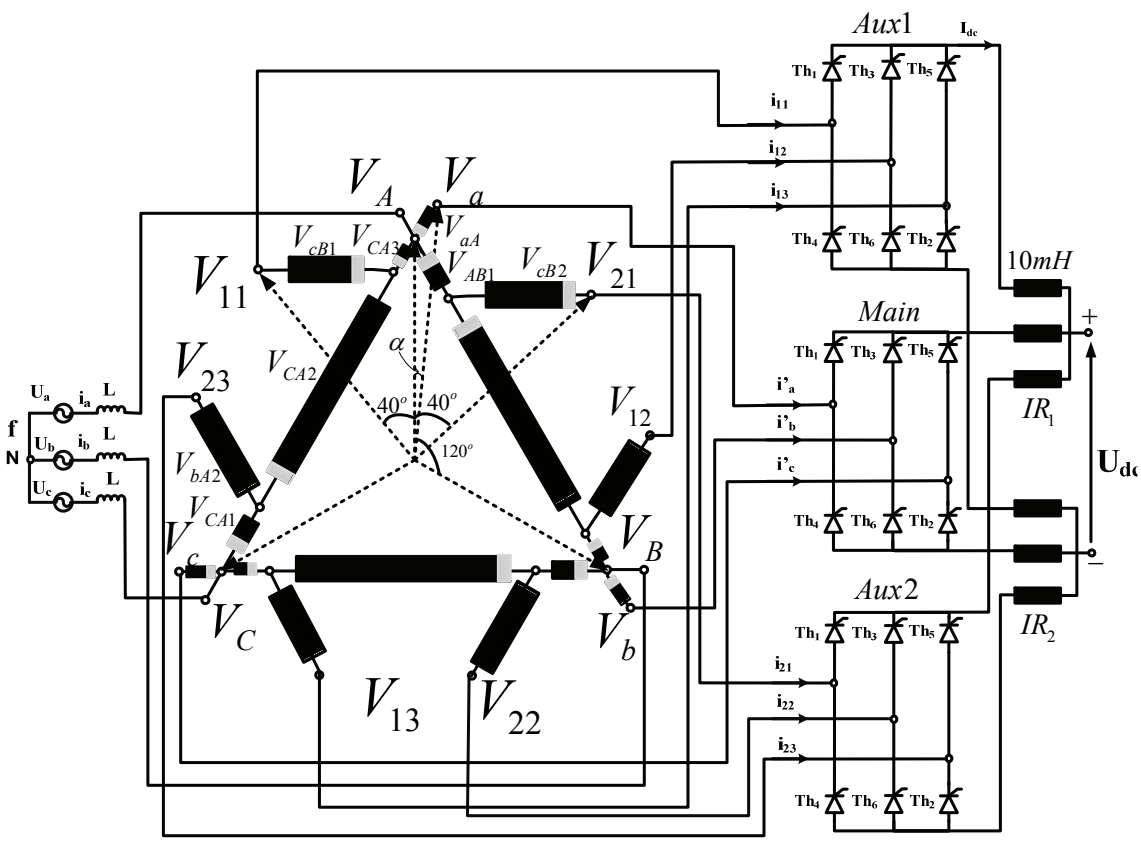

Fig. 2. Asymmetrical delta-connected autotransformer.

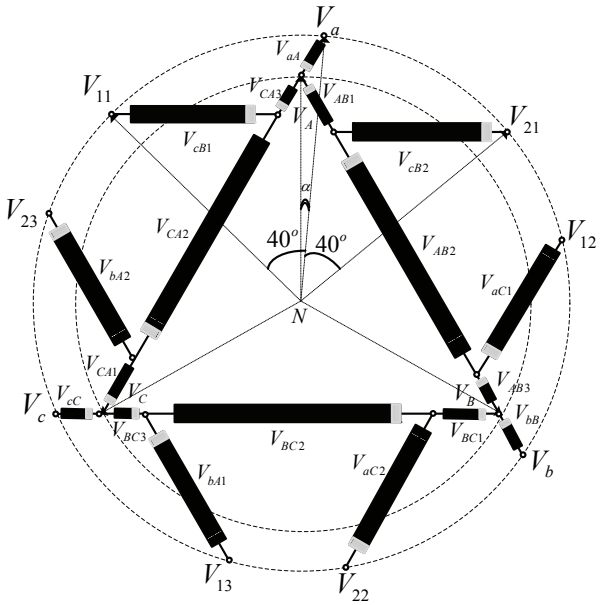

Fig. 3. Representation of a voltage phasor diagram of the step-up delta-connected transformer.

displaced with an angle of 'α'. The displacement between (V_A, V_B, V_C) and (V_{11}, V_{12}, V_{13}) is '40°- α', while the displacement between (V_A, V_B, V_C) and (V_{21}, V_{22}, V_{23}) is '40°+α'. The windings connection limits the amount of circulation of the 3rd harmonic current in them and proves symmetry between the output currents.

The new step-up asymmetrical delta-connected autotransformer using six windings per phase to supply three converters is illustrated in Fig. 2.

The nine secondary voltages related to Fig. 3 are expressed as follows.

$$V_{11} = V_A + V_{CA3} - V_{cB1} \tag{1}$$

$$V_{21} = V_A - V_{AB1} + V_{cB2} \tag{2}$$

$$V_a = V_A + V_{aA} \tag{3}$$

$$V_{12} = V_B + V_{AB3} - V_{aC1} \tag{4}$$

$$V_{22} = V_B - V_{BC1} + V_{aC2} \tag{5}$$

$$V_b = V_B + V_{bB} \tag{6}$$

$$V_{13} = V_C + V_{BC3} - V_{bA1} \tag{7}$$

$$V_{23} = V_C - V_{CA1} + V_{bA2} \tag{8}$$

$$V_c = V_C + V_{cC} \tag{9}$$

Where $V_{ABn} = V_{BCn} = V_{CAn}$ and n=1:3; $V_{aA} = V_{bB} = V_{cC}$; $V_{bA1} = V_{cB1} = V_{aC1}$; and $V_{bA2} = V_{cB2} = V_{aC2}$.

The voltages V_{aA} , V_{CA3} , V_{cB1} , V_{cB2} , V_{AB1} and V_{CA2} are obtained from the rule of the circle circumscribed equilateral

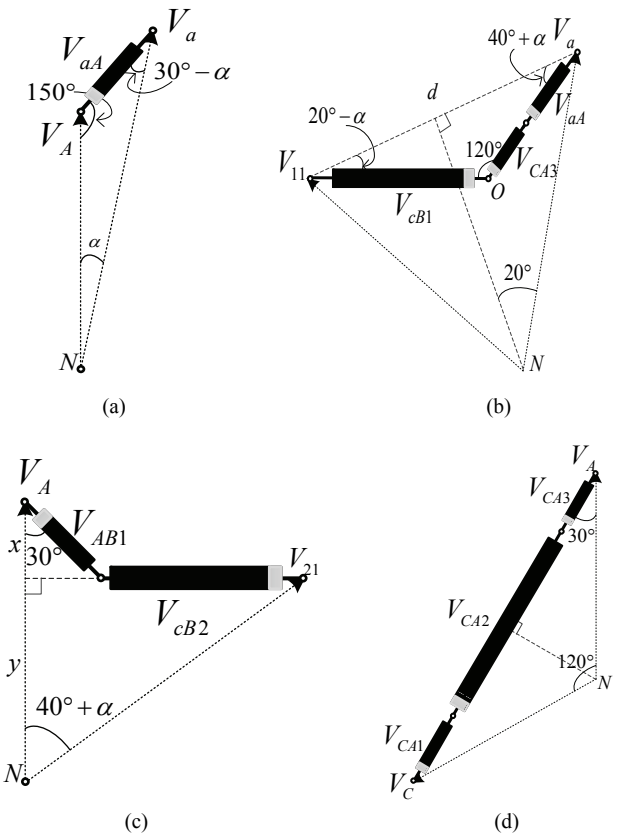

Fig. 4. Vector diagrams.

triangle and sine rule for general triangles.

From the triangle NV_aV_A depicted in Fig. 4(a), the following expression can be written:

$$\frac{V_a}{\sin(150^\circ)} = \frac{V_{aA}}{\sin(\alpha)} = \frac{V_A}{\sin(30° - \alpha)} \tag{10}$$

In Fig. 4(b), from the triangle OVaV11 the expression is given as follow:

$$\frac{V_{CA3} + V_{aA}}{\sin(20^\circ - \alpha)} = \frac{V_{cB1}}{\sin(40° + \alpha)} = \frac{d}{\sin(120°)} = \frac{2*\sin(20°)*V_a}{\sin(120°)} \tag{11}$$

The relations between the angles depicted in Fig. 4(c) can be written as:

$$\cos(30°) = \frac{x}{V_{AB1}} \tag{12}$$

$$\cos(40° + \alpha) = \frac{y}{V_a} \tag{13}$$

$$V_A = x + y = V_a * \cos(40 + \alpha) + V_{AB1} * \cos(30°) \tag{14}$$

$$\sin(40° + \alpha) = \frac{V_{cB2} + z}{V_a} \tag{15}$$

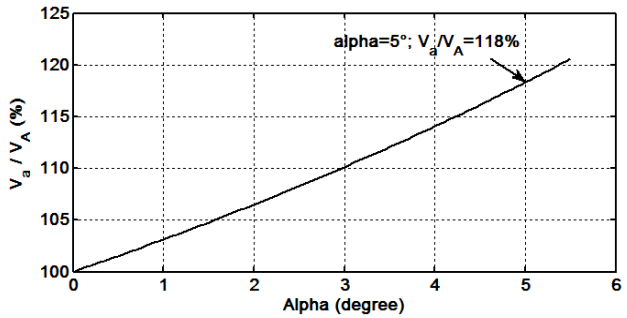

Fig. 5. The ratio $\frac{V_a}{V_A}$ in % versus the angle α.

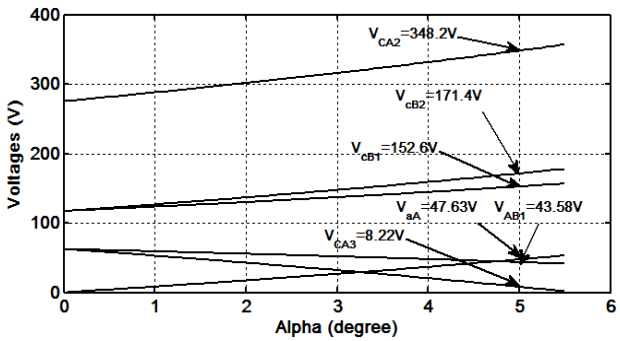

Fig. 6. The six voltage windings versus the angle α.

$$\sin(30°) = \frac{z}{V_{AB1}} \tag{16}$$

From Fig. 4(d), the relation is expressed as follow from the triangle NVAVC:

$$\cos(30°) = \frac{V_{CA1} + V_{CA2} + V_{CA3}}{2 * V_A} \tag{17}$$

Thus, the values of V_a, V_{aA}, V_{CA3}, V_{cB1}, V_{cB2}, V_{AB1} and V_{CA2} are given by Equs. (10)-(17), respectively:

$$V_a = \frac{V_A * \sin(150^\circ)}{\sin(30° - \alpha)} \tag{18}$$

$$V_{aA} = \frac{\sin(\alpha)}{\sin(30° - \alpha)} * V_A \tag{19}$$

$$V_{CA3} = \frac{2\sin(20°) * \sin(20^\circ - \alpha) * V_a}{\sin(120°)} - V_{aA} \tag{20}$$

$$V_{cB1} = \frac{2\sin(20°) * \sin(40° + \alpha) * V_a}{\sin(120°)} \tag{21}$$

$$V_{AB1} = \frac{V_A - V_a * \cos(40 + \alpha)}{\cos(30°)} \tag{22}$$

$$V_{cB2} = V_a * \sin(40 + \alpha) - V_{AB1} * \sin(30°) \tag{23}$$

$$V_{CA2} = 2 * V_A * \cos(30°) - V_{CA1} - V_{CA3} \tag{24}$$

TABLE I
COEFFICIENT OF THE IRON LOSSES IN THE MODEL BEROTTI

Steel material used: AISI 1010	
Hysteresis 'KH'	15,45.10-3 [SI]
Additional 'KE'	3,2.10-3 [SI]
Resistivity	17,6.108 [ohm]
Thickness of sheet metal	0, 5.10-3 [m]
Density	7,85.103[kg / m^3]

According to (18), the step-up voltage is shown in Fig. 5. In this paper, an angle α equal to 5° is chosen to produce nine output voltages equal to 472 V rms for a 400 V input.

The autotransformer is wound on three regular magnetic cores with six windings in each core. For any choice of phase angle α, all of the windings voltages can be determined as shown Fig. 6.

IV. EXPERIMENTAL PROTOTYPE

A laboratory set-up of the proposed asymmetrical nine-phase delta-connected transformer is realized using three-phase laminations EIT series modeled. It is designed using FEA and validated with an experimental prototype realized in the laboratory as shown in Fig. 12. The industry standard of 3D modeling is adopted in the practice of transformer design. With 3D design software, the anisotropy and the non-linearity of the magnetic characteristic BH of the core material is considered. In addition, the distribution of the magnetic flux especially in the portion of the coil (End Region) beyond the window of the core is not possible to calculate in 2D model.
The selection of steel is important to determine the number of turns for each coil. The carbon content allows the magnetic performance of steel, for example steel grade "AISI 1010"with a content of less than 0.1% carbon. According to the BH curve in Fig. 7(b), the relationship of the nonlinearity becomes high at B ≥ 1.5 Tesla. To decrease and switch the eddy current losses in a transformer, the steel core thickness should be reduced. The core is stacked by a lamination of thin electrical steel sheets with a thickness of 0.8 mm or less. These laminations are insulated from each other by a covering of varnish with thickness of about 10-20 μm. The coefficients of the iron losses are reported in Table I.

The appellations of the coils considering the phase AB are shown in Fig. 7(a). To improve the magnetic coupling between the coils, each limb comports six concentrates coils. The geometric parameters of the core and coils are shown in Table II and Table III, respectively.

From the Boucherot theorem Equ. (25), the turn number of the six coils of the proposed autotransformer are calculated and depicted in Table IV.

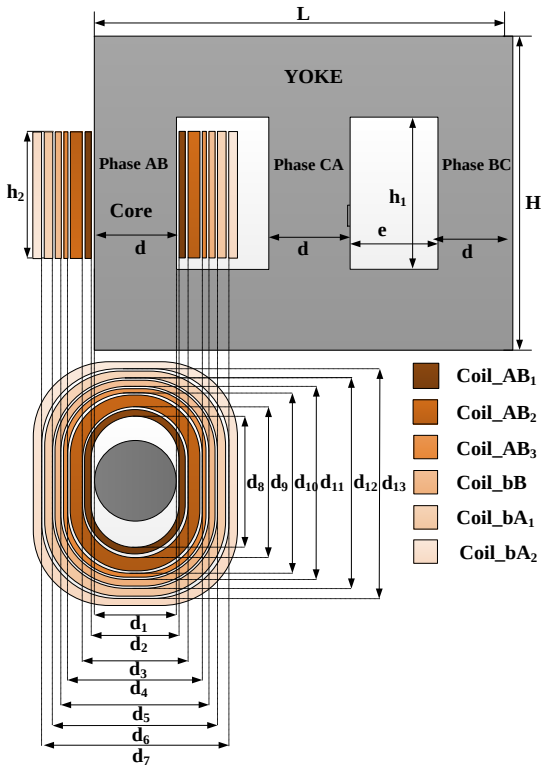

(a)

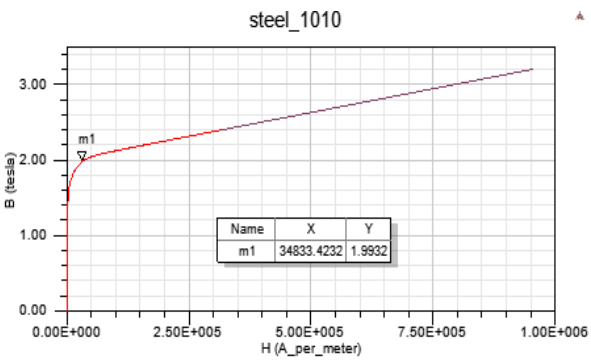

(b)

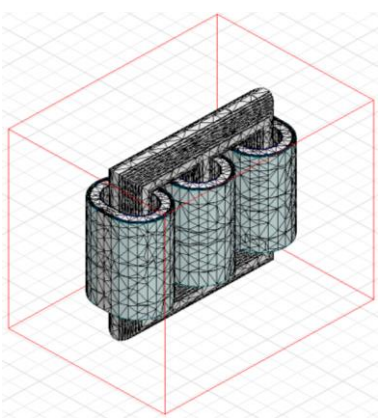

(c)

Fig. 7. Finite element parameters: (a) Three limbs, three phase core and coil type autotransformer; (b) BH Steel 1010. characteristics; (c) 3D results of the meshing of an autotransformer.

TABLE II
CORE PARAMETERS GEOMETRY

Geometry design (mm)					
H	L	d	e	h_1	thickness
200	200	40	40	120	0.5

TABLE III
COIL PARAMETERS GEOMETRY

Geometry design (mm)						
d_1	d_2	d_3	d_4	d_5	d_6	d_7
40	42	43.72	50.48	51.61	53.35	58.33
d_8	d_9	d_{10}	d_{11}	d_{12}	d_{13}	h_2
61	62.72	69.48	70.61	72.35	77.33	115

TABLE IV
WINDINGS PARAMETERS AND COILS TURN NUMBER

	Voltage (V)		Turns number	section
Primary winding	Coil_AB1	43,58	68	0.48mm^2
	Coil_AB2	348,2	544	0.48mm^2
	Coil_AB3	8,22	13	0.48mm^2
Secondary winding	Coil_bB	47,63	74	0.46mm^2
	Coil_bA1	152,6	238	0.46mm^2
	Coil_bA2	171,4	268	0.46mm^2

$$N_{coil} = \frac{V_n}{4,44\,fBS} \tag{25}$$

Where:

V_n: The rms voltage across a winding.

N: The number of turn.

B: The magnetic field peak amplitude (T).

f: The voltage frequency (Hz).

S: A section of one limb magnetic circuit in (m²).

With ANSYS software Maxwell 2D and 3D, the primary windings of delta-autotransformer are connected with the full rated AC external exciting voltages while leaving the secondary windings open. Fig. 7(c) shows three-dimensional result of the auto-transformer meshing with triangle nodes. The asymmetry of the 3D flux distribution (B_x,B_y,B_z) between the phases (AB, CA and BC) during open-circuit operation is shown in Fig. 8. The magnetic distribution in phase (BC) of the core material reveals fully saturable behavior at B≥ 2 Tesla. The magnetizing asymmetry which results in the field currents (H_x,H_y,H_z) in Fig. 9 and the magnetic energy (E_x,E_y,E_z) in Fig. 10 of the three phases, arises due to the mutual magnetic couplings asymmetry between the phases [22]. In addition, core saturation occurs under no-load operation and generates some harmonics in the excitation current. Due to the saturation materials, the relative permeability rises with H to a maximum. Then as it approaches saturation, it inverts and decreases toward one.

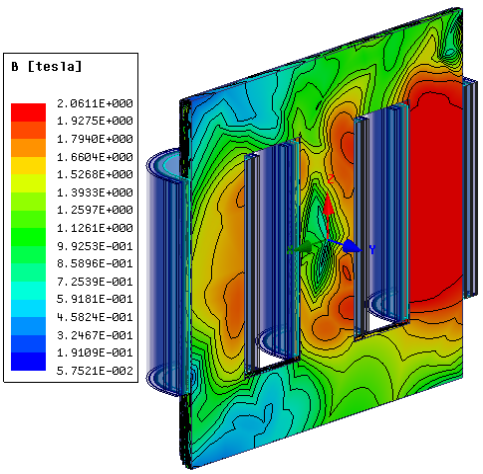

Fig. 8. 3D Magnetic Flux B (Tesla) in the open-circuit condition.

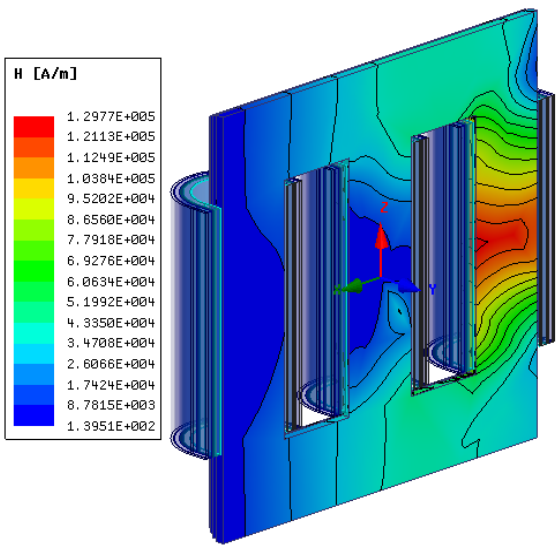

Fig. 9. 3D Field Intensity H (A/m) in the open-circuit condition.

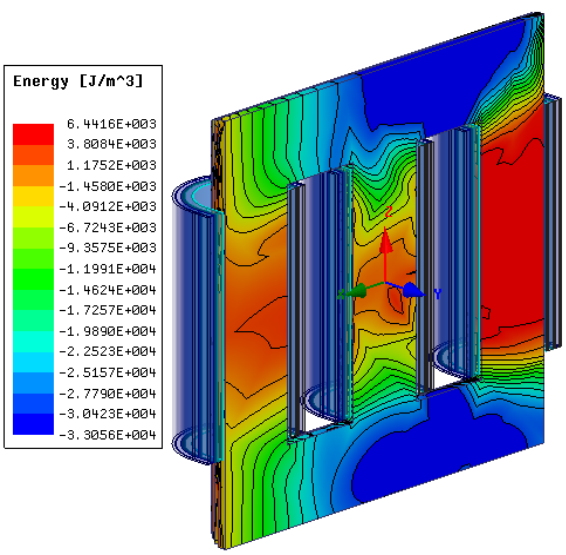

Fig. 10. 3D Magnetic energy (J/m^3) in the open-circuit condition.

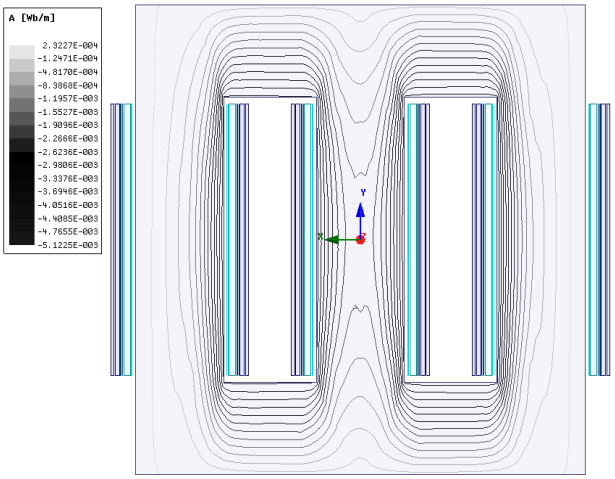

Fig. 11. 2D flux Lines (Wb/m).

The distribution of flux line presented in Fig. 11 shows the field lines concentrated around the limbs of the core transformer and especially around the conductors, where increasing the density of current and voltage is marked.

V. Results and Discussion

Step-up asymmetric delta-connected transformer winding-connection based on an 18-pulse ac-dc converter has been modeled and designed in MATLAB Simulink. This 18-pulse ac-dc converter system is fed by a sinusoidal voltage 400V, 50Hz and connected a nonlinear RLE dc load (R=5Ω, L=20mH). The simulation results are for a 30° firing angle for Thyristor converters.

Fig. 13 shows waveforms of the input voltage and the three sets of balanced voltages systems for one phase. It is observed that the voltage magnitude is equal and symmetric. In addition, it is clear that V_{ab}=1.18*V_{AB}. Moreover, phase displacements of 5° and 40° among the three output three-phase systems can also be verified.

A waveform of the input current is shown Fig. 14 with lower harmonics, which is validated by the harmonic spectrum shown in Fig. 15. It is observed that the line current has a reduced harmonic distortion. The harmonic spectrum, indicates the harmonics order components $18n \pm 1$ **(**for n=1, 2, 3…). The obtained THD is 5.12%. Then it is validated by the experimental outcomes shown in Fig. 16(a), which proves that the input current contains fewer harmonics. The experimental THD is shown in Fig. 16(b) and it is equal to 5.35%.

VI. HV Autotransformer Design with Transportation Restraints

These days, HVDC projects allow for power transmissions of up to 10GW, for an AC network voltage of up to 400kV

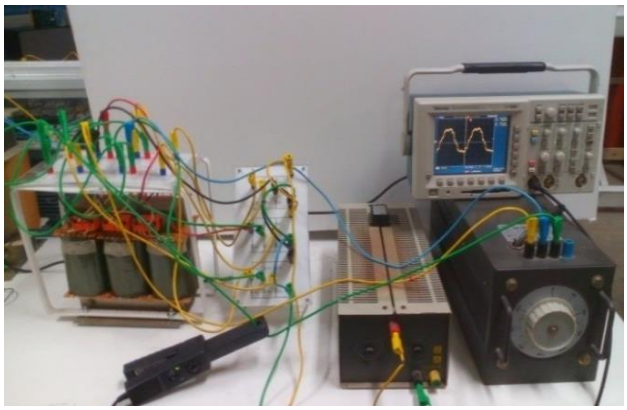

Fig. 12. Experimental setup of an 18 pulse Delta-connected transformer.

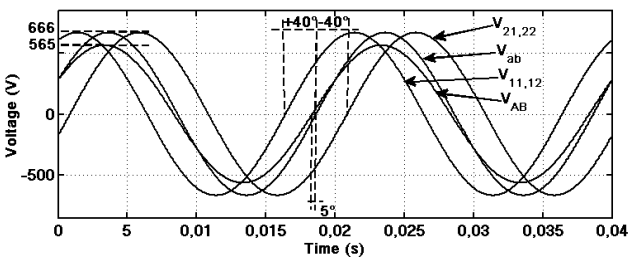

Fig. 13. Line voltage and the achieved three-phase systems.

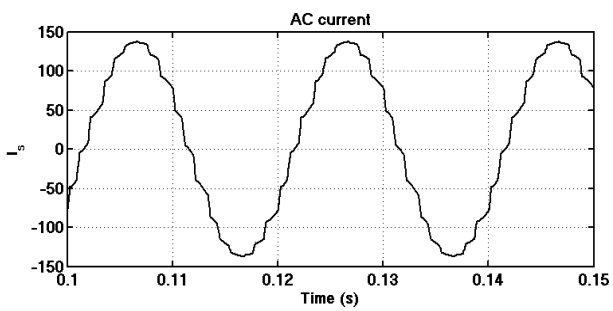

Fig. 14. AC current.

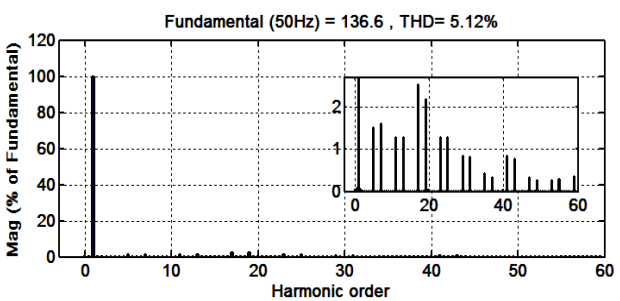

Fig. 15. Harmonic spectrum of the line current.

and a DC voltage of up to ±500kV. The design concept of an 18-pulse step-up asymmetrical delta-connected transformer is principally influenced by transportation restraints such as the dimensions, weight and mode of transportation. A HVDC 18 pulse autotransformer structure can be realized with three sets of single-phase autotransformers with four core limbs (two

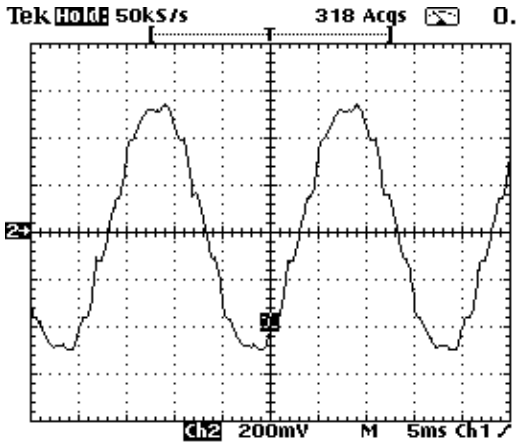

(a)

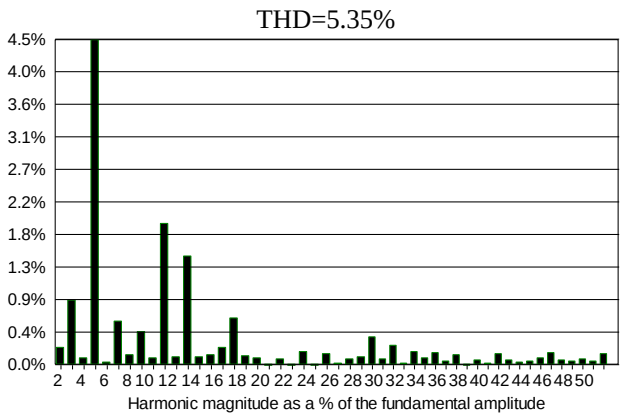

(b)

Fig. 16. Experimental results of the proposed structure: (a) Network current; (b) Harmonic spectrum of the line current.

wound legs and two return legs). In order to increase the magnetic coupling, half of the six concentrates coils are wound on each leg of the two inner limbs, which have twice the cross-sectional area of the two outer limbs.

CRGO core steel is a Cold Rolled Grain Oriented Silicon Steel. The manufacturing transformer core is produced using this type of steel. The maximum flux density of CRGO steel is about 1.9 Tesla. The steel becomes saturated at a flux density equal to 1.9 Tesla.

The transformer windings are exposed to AC and DC dielectric stress between the turn-to-turn, section-to-section, winding-to-winding, winding to core, phase-to-phase, between the leads, from the winding and leads to the constructional parts, and from the bushing to the tank. Therefore, a special insulation assembly is necessary by the selection of the bushings, surge arresters and insulating structure (graded or fully insulated, internal and external clearances, the use of barriers, caps and collars, stress rings, etc.). Furthermore, to resist the DC voltage of the rectifier, special leads systems connecting the turrets and windings should be installed. Different standards are applied to the HVDC transformer design:

- IEC 61378-2 (1.0) 2001-02 Converter Transformers – Part 2 Transformers for HVDC Applications.
- IEC 61378-3 Converter Transformers – Part 3 Application Guide for Converter Transformers.
- IEC 62199: 2004-05 Bushings for DC Application.
- IEEE Std. C57.129-1999 General Requirements and Test Code for Oil Immersed HVDC Converter Transformers.
- IEEE Std. 1158-1991 (R 1996) Recommended Practice for Determination of Power Losses in HVDC Converter Stations.

VII. CONCLUSIONS

In this paper, a step-up asymmetrical delta-connected autotransformer using an interphase reactor to guarantee parallel connection in the dc side between the converters has been presented. The design of the autotransformer structure has been studied and simulated it in MATLAB Simulink. In addition an experimental prototype has been build and studied in the laboratory. The obtained results show that the use of the asymmetric autotransformer gives a better simulated THD equal to 5.12% and an experimental THD equal to 5.35% of the supply current. This new structure ensures symmetry between the output voltages and gives an output current with the same amplitude. Moreover, this design produces a waveform of the dc output voltage that contains 18 undulations, which provides the 18-pulse rectification that offers a greater flexibility in terms of the transit control of energy and a significant harmonics reduction in HVDC applications. Finally, future works will focus on other topologies that give better THD such as the design of another auto-connected with another special coupling.

REFERENCES

[1] D. A. Paice, "Power electronic converter harmonics: multipulse methods for clean power," *IEEE Press*, 1996.

[2] S. Pyakuryal and M. Matin, "Harmonic for a 6-pulse rectifier," *IOSR Journal for engineering*, Vol. 3, pp. 2278-8719, Mar. 2013.

[3] F. Meng, L. Gao, S. Yang, and W. Yang, "Effect of phase-shift angle on a delta-connected autotransformer applied to a 12-pulse rectifier," *IEEE Trans. Ind. Electron.*, Vol. 62, No. 8, pp. 4678-4690, Aug. 2015.

[4] B. Singh, G. Bhuvaneswari, and V. Garg, "Harmonic mitigation using 12-pulse AC-DC converter in vector-controlled induction motor drives," *IEEE Trans. Power Del.*, Vol. 21, No. 3, pp. 1483-1492, Jul. 2006.

[5] B. Singh, G. Bhuvaneswari, and R. Kalpana, "Autoconnected transformer-based 18-pulse ac-dc converter for power quality improvement in switched mode power supplies," *IET Power Electron.*, Vol. 3, No.4, pp. 525-541, Jul. 2010.

[6] D. A. Paice, "Optimized 18-pulse type ac–dc or dc–ac converter system", U.S. Patent No. 5124904 A, Jun. 23, 1992.

[7] C. Kim and S. Lee, "Redundancy determination of HVDC MMC modules," *Electronics*, Vol. 4, No. 3, pp 526-537, Aug. 2015,

[8] K. M. Kim, J. H. Kim, D. H. Kim, B. M. Han, and J, Y, Lee, "Improved pre-charging method for MMC-based HVDC systems operated in nearest level control," *J. Power Electron.*, Vol. 17, No. 1, pp. 127-135, Jan. 2017.

[9] A. Hassanpoor, Y. J Häfner, A. Nami, and K. Vinothkumar, "Cost-effective solutions for handling DC faults in VSC HVDC transmission," *EPE*, pp. 5-9, 2016.

[10] J. Häfner and B. Jacobson, "Proactive hybrid hvdc breakers a key innovation for reliable hvdc grid," *in Cigrésymposium*, pp. 13-15, Sep. 2011.

[11] A. Mokhberdoran, N. Silva, H. Leite, and A. Carvalho, "Unidirectional protection strategy for multi-terminal HVDC grids," *Trans. Environment and Electrical Engineering*, Vol. 1, No. 4, 2016.

[12] J. Vobecky, T. Stiasny, V. Botan, K. Stiegler, U. Meier, and M. Bellini, "New thyristor platform for UHVDC (>1 MV) transmission," *International Exhibition and Conference for Power Electronics, Intelligent Motion, Renewable Energy and Energy Management*, pp. 20-22, May. 2014.

[13] B. Sheng, H. O. Bjarme, and H. Johansson, "Reliability enhancement of HVDC transmission by standardization of thyristor valves and valve testing," *6th Int. Conf. on Power T&D Technolog*, Nov. 10-12, 2007.

[14] B. L. Sheng, H. O. Bjarme, O. Saksvik, L. Carlsson, and R. Ruderval, "Modern thyristor valves and HVDC transmission technologies," *Trans. High Voltage Apparatus*, Vol. 39, No. 6, pp.47-50, 2003.

[15] M. B. Baherman and B. K. Johnson, "The ABCs of HVDC transmission technology," *IEEE Power Energy Mag.*, Vol. 5, No. 2, Apr. 2007

[16] B. A. Arafet and B. A. Faouzi, "Auto-connected transformer with 40° phase shifting for harmonic elimination," *Int. J. Signal Imaging Syst. Eng.*, Vol. 9, Nos. 4/5, pp. 233-241, 2015.

[17] E. N. A. Matus, "Analysis and design of new harmonic mitigation approaches," PhD. thesis, Texas A&M University, 2012.

[18] D. A. Paice, "Nine-phase step-up/step-down autotransformer," U.S. Patent No. 7274280 B1, Sep.25, 1992.

[19] D. Hammond, "Autotransformer", U.S Patent No. 5619407 A, Apr.8, 1997.

[20] G. R. Kamath, "Autotransformer-based system and method of current harmonic reduction in a circuit," U.S. Patent No. 6861936, Mar. 1, 2005.

[21] K. Oguchi, "Autotransformer-based 18-pulse rectifiers without using dc-side interphase transformers: Classification and comparison," *International Symposium Power Electronics, Electrical Drives Automation and Motion SPEEDAM*, pp.760-765, Jun. 2008.

[22] R. E. Perez, S. V. Kulkarni, N. K. Kodela, and J. C. O. Galvan, "Asymmetry during load-loss measurement of three-phase three-limb transformers," *Power Engineering Society General Meeting IEEE*, 2007.

Arafet Ben Ammar was born in Tunis, Tunisia, on December 7, 1988. He received his B.S. degree in Electronics, Electrical Engineering and Automation and his M.S. degree in Electrical Engineering (course conversion and treatment of electrical energy) from the National School of Engineering of Tunis (ENIT), Tunis, Tunisia, in 2010 and 2012, respectively, where he is presently working towards his Ph.D. degree in Electrical Engineering in collaboration with the National Institute of Applied sciences and Technology of Tunis (INSAT), Tunis, Tunisia. His current research interests include power electronics and machine modeling, electrical networks and power converters.

Faouzi Ben Ammar was born in Tunis, Tunisia, on May 15, 1962. He received his B.S. degree in Electrical Engineering from National Engineering School of Monastir (ENIM), Monastir, Tunisia, in 1987; and his M.S. and Ph.D. degrees from the INP-ENSEEIHT, National Polytechnic Institute of Toulouse, Toulouse, France, in 1989 and 1993, respectively. From 1993 to 1998, he worked as an Engineer in the Alstom Company, Belfort, France, where he was involved in the development of control drive systems. In 1998, he became an Assistant Professor in the National Institute of Applied Sciences and Technology of Tunis (INSAT) Tunis, Tunisia, where he has been a HDR and a professor of power electronics since 2004. His current research interests include power electronics, machine modeling, control induction motor drives, pulse width modulation, multilevel inverters, active filters, reliability and RMAS analysis.